sustainability

MDPI

Article

Design and Numerical Simulation of the Headworks in the Shizuishan Section of the Yellow River

Mingyang Liu [1], Suiju Lv [1,*], Qiao Qiao [2] and Lulu Song [3]

[1] School of Civil Engineering, North Minzu University, Yinchuan 750021, China
[2] Department of Architecture, Lvliang University, Lvliang 033400, China
[3] School of Civil and Hydraulic Engineering, Ningxia University, Yinchuan 750021, China
* Correspondence: 2005060@nmu.edu.cn; Tel.: +86-137-095-853-70

Abstract: Irrigation water for agriculture in Ningxia during the summer is primarily sourced from the Yellow River self-flow irrigation region. However, the water conveyance system in this region is significantly influenced by hydrodynamic factors, morphological factors, human factors, and the infrastructure used for social purposes, all of which directly impact the irrigation water utilization coefficient. In order to improve the irrigation water utilization coefficient, reduce suspended sediment deposition in the water conveyance channels, and mitigate negative effects on the water supply system, this study implemented a sediment diversion system at the channel head. This is expected to increase water usage efficiency to a certain degree. Using actual data on hydrodynamic factors from the Shizuishan section of the Yellow River in Ningxia, a two-dimensional numerical simulation was performed, and a two-dimensional hydrodynamic model and sediment model of the Shizuishan section of the Yellow River in Ningxia were developed using MIKE 21. The water conveyance method at the channel head was simulated under two different operating conditions. Results indicated that compared to operating condition 1, operating condition 2 had a beneficial effect on diverting and reducing sediment at the fish mouth of the channel head: the sediment accumulation thickness of one day in operating condition 1 was 0.16 m, 0.003 m, 0.15 m, and 0.21 m under actual flow, scenario 1, scenario 2, and scenario 3, respectively; whereas in operating condition 2, the sediment accumulation thickness of one day was 0.11 m, 0.001 m, 0.09 m, and 0.12 m under the same conditions, respectively. Additionally, as the computation period lengthened, the sediment accumulation thickness of operating condition 2 was significantly smaller than that of operating condition 1. In conclusion, operating condition 2 is superior for the design of the channel head in the Yellow River self-flow irrigation region.

Keywords: the Yellow River Irrigation District; numerical simulation; river erosion; sediment movement; diversion channel

Citation: Liu, M.; Lv, S.; Qiao, Q.; Song, L. Design and Numerical Simulation of the Headworks in the Shizuishan Section of the Yellow River. *Sustainability* **2023**, *15*, 4564. https://doi.org/10.3390/su15054564

Academic Editors: Hamza Gabriel, Songhao Shang, Qianqian Zhang, Dongqin Yin and Magdy Mohssen

Received: 22 January 2023
Revised: 23 February 2023
Accepted: 24 February 2023
Published: 3 March 2023

1. Introduction

Agricultural modernization in Ningxia has led to the need for more diverse and stronger infrastructure in irrigation areas. As the focus of irrigation construction shifts, there is a need to improve quality and efficiency. One challenge in these areas is the low water level and high sand content of the Yellow River, which causes sediment accumulation in the channels of self-flow irrigation areas and decreases the irrigation water utilization coefficient. Researchers from within and outside China have studied the water and sediment movement in these sedimentary basins to develop models and management strategies that aim to improve the irrigation water utilization coefficient and enhance the ecological environment.

At the head of the diversion channel are critical hydraulic structures that serve several purposes. On one hand, they divert water from rivers into channels to fulfill the needs of water resource projects such as irrigation, hydropower generation, and domestic water

supply [1,2]. On the other hand, they prevent the entry of coarser sediment particles into bends, thus reducing erosion and sedimentation, and ensuring normal bend operation. As a result, numerous scholars have conducted extensive research on the specific hydrodynamic and sediment transport characteristics of headworks bends, as well as the evolution patterns of the riverbed [3,4]. Sediment in channels is a significant factor that controls the morphological and hydraulic characteristics of the riverbed [5,6], and the grain size of the sediment significantly affects water flow resistance, sediment transport, and the intensity of riverbed erosion [7,8]. Furthermore, the sediment transport capacity of rivers can vary with changing downstream hydraulic conditions, and the difference in sediment transport capacity during flood events can cause changes in riverbed material. In turn, changes in riverbed material can result in irregular fluctuations in the bed surface and sediment transport, which are mechanisms of sediment transport in rivers [9–12].

As the mechanisms of river sediment transport continue to be studied by researchers, Bognold [13] developed equations for the calculation of suspended sediment and bedload sediment transport rates, which have significantly advanced our understanding of water and sediment dynamics. Chen et al. [14] conducted an analysis of annual runoff and sediment sequences, providing insight into the downstream impacts of water conservancy projects, including gradual weakening of runoff and sedimentation from upstream to downstream. An et al. [15] examined hydrodynamic data from the segment of the Yellow River Basin spanning from Ningxia to Inner Mongolia since the 1960s, determining that channel erosion and sedimentation are primarily the result of both mainstream and tributary processes. Krishnappan et al. [16] investigated the relationship between sediment particle size and settling velocity in the sedimentation process; smaller-grained sediments in rivers are more susceptible to deposition and accumulation due to their reduced volume, which results in a lower level of erosive force exerted by the water flow. The river current is composed of two water layers with varying velocities, with higher water speeds leading to smaller suspended particle sizes. As the particle size decreases, the likelihood of its being transported and subsequently deposited by the water flow increases. Therefore, smaller-grained sediment is more readily deposited and accumulated in rivers. Finally, Jin et al. [17] analyzed sediment initiation and water flow sediment carrying capacity, and investigated the advancement patterns of sediment in the Yellow River irrigation area.

With the advancement of computational capabilities and the integration of modern technologies, computer-aided visualization techniques have been employed to investigate the hydrodynamic behavior and sediment transport characteristics in irrigation channels [18–20]. In this context, Soulis [21] conducted a study on the Mornos drainage canal in Athens, utilizing numerical simulations to reproduce the mechanisms of channel damage in vulnerable areas. Oyarce [22] employed computational fluid dynamics (CFD) models to numerically evaluate the hydrodynamic characteristics of agricultural drainage channels with varying geometries, and analyzed the temporal variations in flow direction, velocity, relative soil moisture content and head pressure during the drainage process. Alomari [23] conducted physical experiments to investigate the effects of the channel angle on erosion and deposition in rivers at angles of 30°, 45°, 60°, 75°, and 90°. The results indicated that as the angle of the channel increased, the thickness of the deposited sediment decreased, with the smallest amount observed at 90°. However, it was observed that solely altering the angle of the channel had a limited impact on the hydrodynamic characteristics within the channel, and was not found to be an effective means of reducing sedimentation and erosion. The utilization of fish mouth diversion structures at the Dujiangyan irrigation hub leverages the principle of fish mouth diversion to optimize the distribution of water flows [24]. This study aims to investigate the impact of the bedform on sediment transport in the river channel and to adjust unfavorable flow conditions by changing the hydraulic characteristics of the river through the construction of fish mouth engineering. The Yellow River engineering channel serves as the subject of this study and the characteristics of fish mouth diversion and sedimentation at Dujiangyan are taken into consideration. Numerical simulation methods are employed to design various operating scenarios. The scouring and

silting characteristics are analyzed under different conditions, reflecting different periods of water and sediment characteristics as well as incoming water and sediment conditions.

The integration of SMS software and MIKE21 software can enhance the efficiency and accuracy of river flow and hydrodynamic simulations [25]. In this study, the SMS software was utilized to partition the grid of the study region under various operational conditions. The generated grid files were imported into the MIKE 21 software, where the water dynamics and sediment transport modules were coupled to simulate the evolution of channel sediment. The sediment accumulation patterns were analyzed and the changes in channel sediment under different scenarios and operational conditions were compared in order to identify the optimal operational condition.

2. Materials and Methods

2.1. Introduction to the Study Area

The Yellow River Diversion Project is a significant engineering project aimed at ensuring the ecological water use of the people living along the route. The annual average flow of the Yellow River in Ningxia can reach 4 billion m3, with the majority of this water being used for agricultural irrigation. The irrigation period during the summer and autumn lasts approximately 40–50 days, while the winter period lasts approximately 10–15 days, resulting in a total irrigation period of approximately 50–60 days per year. The study area is located in the Shizuishan section of the Yellow River in Ningxia, with a length of 4 km (as depicted in Figure 1a). In order to measure the hydrodynamic elements of this region, acoustic Doppler profilers, GPS-RTK systems, and laser grain size distribution instruments were utilized on 20 October 2017, 20 October 2018, 20 October 2019, and 20 October 2020. The present study utilizes data collected on October 20, 2020, as an example, with the MIKE21 software being utilized to interpolate and generate a 3D view of the region based on the measurements taken at 10 different cross-sections (as shown in Figure 1b).

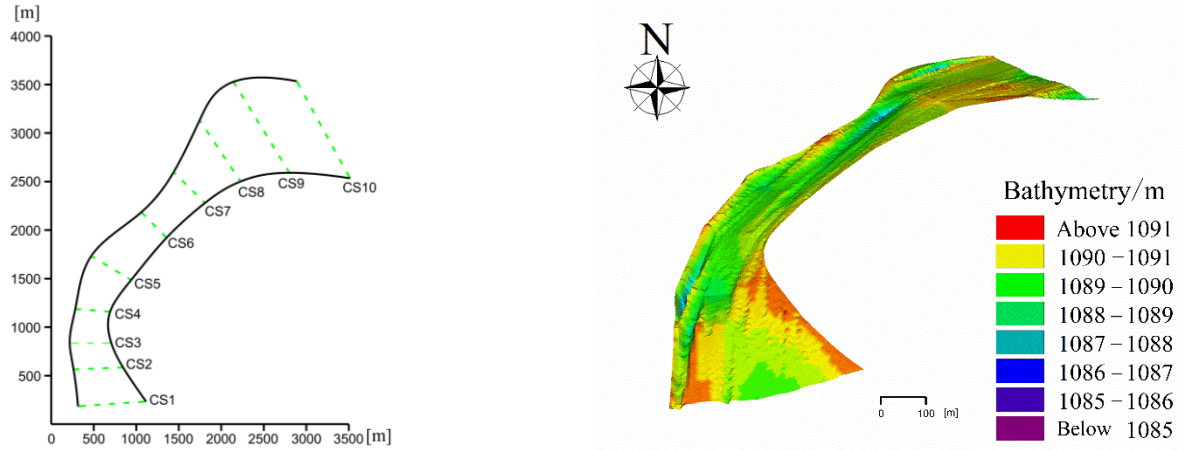

(**a**) (**b**)

Figure 1. Diagram of measurement area, (**a**) Section division of measurement area; (**b**) 3D view of measurement area.

2.2. Mathematical Modelling

The present study employs a grid-based approach to evaluate the hydrodynamic characteristics of a water intake channel in different operating conditions. Surface Water Modeling System (SMS) software was utilized to partition the research region into grids, which were subsequently imported into MIKE 21 for analysis using the hydrodynamic module and sediment transport module. The sediment transport module is based on the calculations from the hydrodynamic module.

The present study employs a two-dimensional hydrodynamic model and a non-viscous mud–sediment coupling model to investigate the study region numerically. The model is founded upon the incompressible Reynolds-averaged Navier–Stokes equations,

comprising the continuity equation, the x direction momentum equation, and the y direction momentum equation.

Hydrodynamic module principle

$$\frac{\partial h}{\partial t} + \frac{\partial h\overline{v}}{\partial x} + \frac{\partial h\overline{v}}{\partial y} = hS \tag{1}$$

The momentum equation in the X direction is

$$\begin{array}{l} \frac{\partial h\overline{u}}{\partial t} + \frac{\partial h\overline{u}^2}{\partial x} + \frac{\partial h\overline{u}\overline{v}}{\partial y} = f\overline{v}h - gh\frac{\partial \eta}{\partial x} - \frac{h}{\rho_0}\frac{\partial Pa}{\partial x} - \frac{gh^2}{2\rho_0}\frac{\partial \rho}{\partial x} + \frac{\tau_{sx}}{\rho_0} \\ -\frac{\tau_{bx}}{\rho_0} - \frac{1}{\rho_0}\left(\frac{\partial S_{xx}}{\partial x} + \frac{\partial S_{xy}}{\partial y}\right) + \frac{\partial}{\partial x}(hT_{XX}) + \frac{\partial}{\partial y}(hT_{xy}) + hU_sS \end{array} \tag{2}$$

The momentum equation in the Y direction is

$$\begin{array}{l} \frac{\partial h\overline{v}}{\partial t} + \frac{\partial h\overline{v}^2}{\partial x} + \frac{\partial h\overline{u}\overline{v}}{\partial y} = -f\overline{v}h - gh\frac{\partial \eta}{\partial y} - \frac{h}{\rho_0}\frac{\partial Pa}{\partial y} - \frac{gh^2}{2\rho_0}\frac{\partial \rho}{\partial y} + \frac{\tau_{sy}}{\rho_0} \\ -\frac{\tau_{bx}}{\rho_0} - \frac{1}{\rho_0}\left(\frac{\partial S_{yx}}{\partial x} + \frac{\partial S_{yy}}{\partial y}\right) + \frac{\partial}{\partial x}(hT_{XX}) + \frac{\partial}{\partial y}(hT_{xy}) + hV_sS \end{array} \tag{3}$$

where t represents the time variable, while h is the total water depth. The x and y variables represent the coordinates in a Cartesian coordinate system. The u and v variables represent the velocity components in the x and y directions, respectively. S refers to the source term, while f denotes the Coriolis force. The g represents the acceleration due to gravity. The variable d denotes the static water depth, while represents the density of water. S_{xx}, S_{xy}, and S_{yy} represent the components of the radiation stress, and Us and V_s represent the flow velocities of the water flow associated with the source term.

The non-cohesive sediment transport calculation is based on a two-dimensional hydrodynamic model that considers a single flow event. The calculation employs comprehensive sediment transport theory to determine the concentrations of suspended and bed load sediments.

Control equation of sediment transport model:

$$\frac{\partial \overline{c}}{\partial t} + u\frac{\partial \overline{c}}{\partial x} + v\frac{\partial \overline{c}}{\partial y} = \frac{1}{h}\frac{\partial}{\partial x}\left(hD_x\frac{\partial c}{\partial x}\right) + \frac{1}{h}\frac{\partial}{\partial y}\left(hD_y\frac{\partial c}{\partial y}\right) + Q_LC_L\frac{1}{h} - S \tag{4}$$

where $\overline{c}$ is the average sediment concentration in the water depth direction (kg/m^3), h is the water depth (m), D_x and D_y are the dispersion coefficients in the x and y directions, respectively (m^2/s), Q_L is the single wide source term flow in the horizontal direction (m^3/s/m^3); this source can be from a single location, such as a stream or river, or from multiple locations that contribute to the sediment transport in a similar manner; C_L is the source sediment concentration, g/m^3, and S is the scouring/silting item (representing any additional sources or sinks of sediment) kg/m^3/s.

2.3. Model Establishment and Parameter Calibration

Terrain data for the study region were processed using SMS software, with boundary attributes defined as open and land boundaries. The upstream open boundary extended 701 m in length and contained 48 nodes, while the downstream open boundary was 1004 m long with 78 nodes. The study region was divided into 15,665 unstructured triangular grid cells, with a grid resolution of 10 m and a minimum angle of 30°, as depicted in Figure 2. Elevation data were based on the 1985 Chinese elevation datum and the 1954 Beijing coordinate system was used for plane coordinates.

In the hydrodynamic module, the annual coefficient of the eddy flow is 0.28; the roughness coefficient of the river bed is calculated using the Manning coefficient, resulting in a value of 36 m$^{1/3}$/s. In the sediment module, flocculation settling is selected as the settling velocity for the suspended sediment, with a rate of 0.01 kg/m^3 and a density of 2650 kg/m^3 for the sediment.

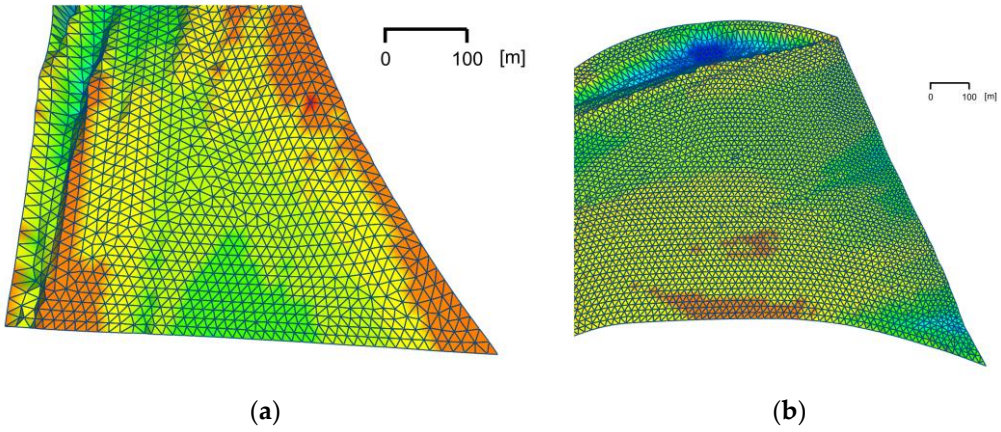

(**a**) (**b**)

Figure 2. Schematic diagram of the gridding of the measurement area, (**a**) Schematic of grid division in upstream study area; (**b**) Schematic of grid division in downstream study area.

2.4. Model Validation

The present study aims to assess the hydrodynamic and sedimentary characteristics of the Shizuishan section of the Yellow River using the hydraulic and sediment modules, respectively, in 2.2.2 and 2.2.3 as of 20 October 2020. The hydraulic data used in this study were obtained from in situ measurements carried out in the study area. The flow velocity and direction were determined through the use of acoustic Doppler profilers, the sediment concentration was estimated using laser particle size distribution instruments, and the water surface elevation was determined using GPS-RTK measurements. The upstream flow rate was set to 1861.5 m^3, based on the measured data, and the downstream elevation was set to 1092.3 m. For the sediment module, the upstream sediment concentration was 1.25 kg/m^3, and the median grain size was 0.15 mm.

The present study validated the hydrodynamic elements and sediment content of cross-sections CS4, CS5, CS6, and CS7, as the design of the water channel is situated between cross-sections CS5 and CS6. The results, shown in Figure 3a, demonstrate that the simulated flow velocity exhibits a similar trend to the measured flow velocity, with a maximum deviation of 0.37 m/s. Similarly, the sediment content in Figure 3b exhibits a maximum deviation of 0.21 kg/m^3. These results indicate that the model used in this study is reliable for simulation purposes, as the fitting error is minimal for both flow velocity and sediment content.

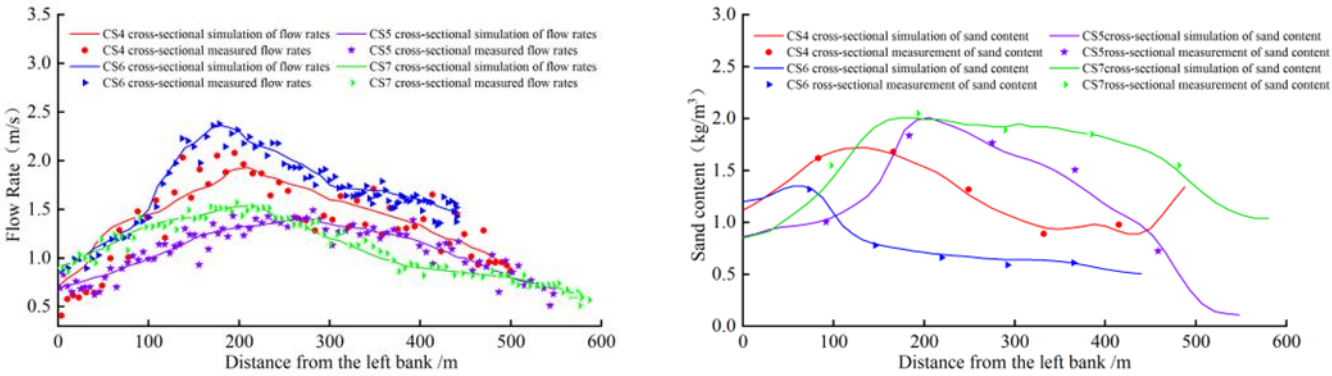

(**a**) (**b**)

Figure 3. Typical section simulation validation chart, (**a**) Typical section flow velocity validation chart; (**b**) Typical section sediment concentration validation chart.

3. Results

3.1. Experimental Design

3.1.1. Design for Working Conditions

To mitigate the negative impact of sediment on channel sedimentation in self-flow irrigation areas, two different operating conditions were designed based on the principle of fish mouth diversion and sediment reduction at the Dujiangyan water conservancy hub. A fish mouth is a specialized architectural structure designed to manage the velocity and orientation of fluidic currents (as shown in Figure 4). This study investigated the utilization of the fish mouth with a diminutive arch-shaped geometrical configuration, situated near the concave bank of the river channel, thus segmenting the river into an internal and external flow path. The fluidic flow entering the arch-shaped space through the upper portion of the fish mouth experienced a reduction in velocity, while the fluidic flow entering through the lower portion produced a robust fluidic current. Consequently, the fish mouth serves as a means to optimize fluidic distribution and effectively modulate fluidic velocity and orientation. Using MIKE 21 software, the erosion dynamics of the two operating conditions under similar upstream hydrodynamic conditions were simulated. Operating Condition 1 consisted of a direct water channel with a sediment blocking crest at the head (as depicted in Figure 4a), 100 m wide, and a channel 800 m long and 20 m wide with a longitudinal gradient of 1‰. The head of the channel employed a leaky bucket design to increase the drainage volume. Operating Condition 2 was similar to Condition 1, but with the addition of a fish mouth at the head of the channel. The sediment blocking crest connected to the natural river channel was 150 m wide and the outlet was 100 m wide. The fish mouth was located on the upper side of the bend of the leading river and was followed by a flying sand weir (as depicted in Figure 4b), 1093 m in elevation and 50 m wide. The fish mouth divided the flow into inner and outer sections, with the inner section being 150 m wide and the outer section being 100 m wide.

The design area was gridded using SMS software (as shown in Figure 5). In Condition 1 (as depicted in Figure 5a), the node spacing within the channel was set at 10 m, with a closer spacing of 5 m at the channel head to enhance the fidelity of this region. In Condition 2 (as shown in Figure 5b), the node division within the channel remained unchanged, but the node spacing in the vicinity of the fish mouth was decreased to 5 m in order to accurately reproduce the hydrodynamic and erosion dynamics in this area.

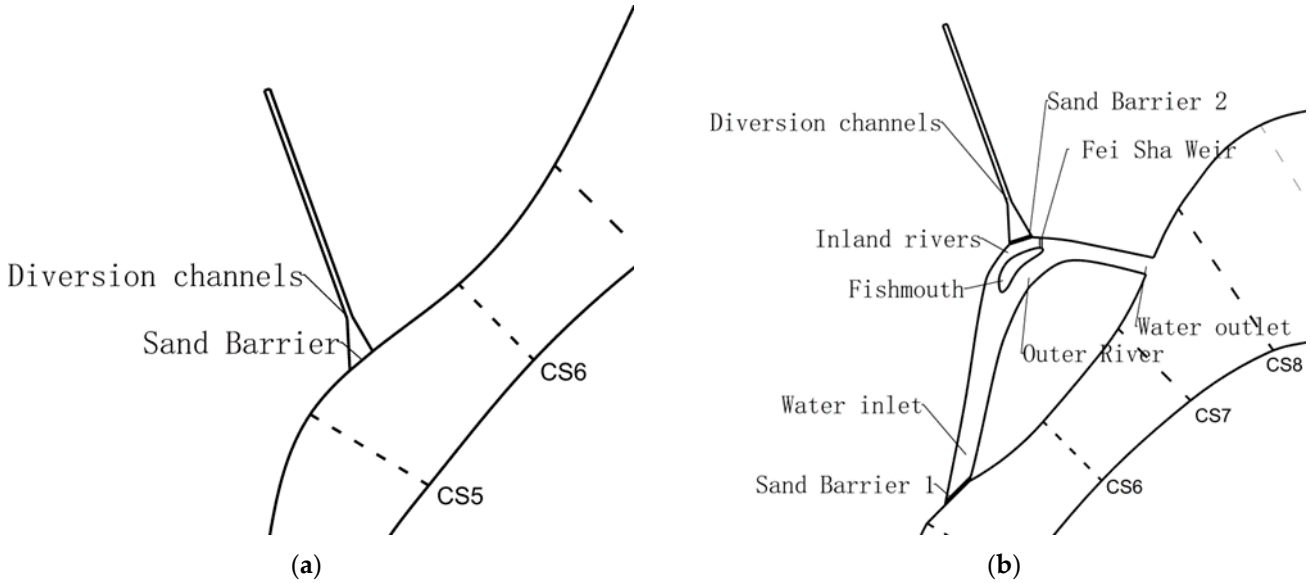

Figure 4. Design diagram of operating conditions, (**a**) Design schematic diagram of Operating condition 1; (**b**) Design schematic diagram of Operating condition 2.

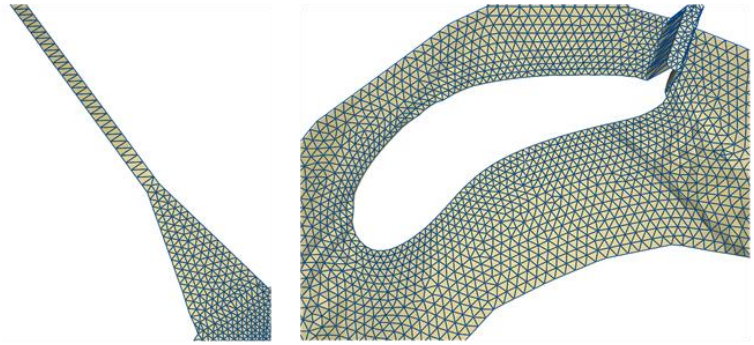

(**a**) (**b**)

Figure 5. Design area grid division map, (**a**) Grid division of water diversion channel; (**b**) Grid division of fish mouth.

3.1.2. Scenario Setting

According to the temporal distribution of irrigation in the Shizuishan section of the Yellow River in Ningxia, flow is typically concentrated from July to October and ranges from 1000 to 2000 m^3/s. However, runoff exhibits dynamic changes due to climatic factors. Therefore, this study establishes three scenarios based on variations in the runoff: Scenario 1 with a flow of 1000 m^3/s, Scenario 2 with a flow of 1500 m^3/s, and Scenario 3 with a flow of 2000 m^3/s.

3.1.3. Fish Mouth Flow Field Distribution

To investigate the spatial distribution of the water flow near a fish mouth, a simulation was conducted to examine the flow field at the fish mouth and the head of a channel under measured flow rates. As illustrated in the flow field vector distribution in Figure 6, the flow field in the outer river exhibits a lower intensity compared to that in the inner river, with flow velocities ranging from 0.2 to 0.48 m/s in the outer river and 0.8 to 0.9 m/s in the inner river, indicating that the outer river exhibits lower kinetic energy and weaker sediment-carrying capacity. At a discharge of 1861.5 m^3/s, the water surface elevation near the sand-ejecting weir is 1092.8 m and a vortex–like backflow is formed between the upstream and the head of the channel. Upon a further increase in the flow rate to the critical value, the water flow overflows the sand-ejecting weir and the sediment is entrained and transported downstream. Condition 2 reproduces the operation of the Dujiangyan water conservancy hub, including the functions of water diversion from the outer river and water discharge from the inner river in an artificial channel, which can be utilized for the purpose of simulation in this study.

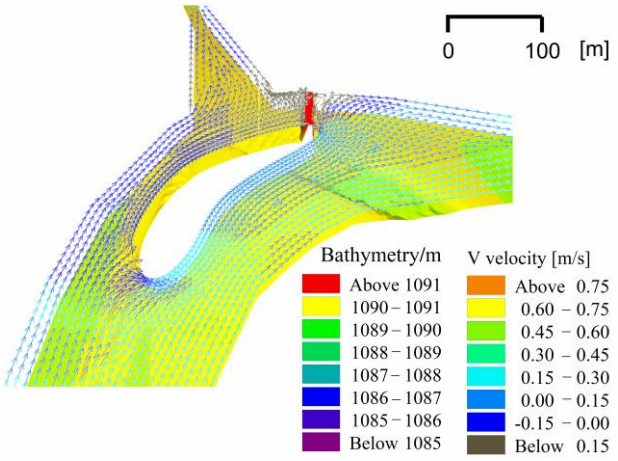

Figure 6. Vector map of flow distribution at the fish mouth.

3.2. Erosion of Diversion Channels at Different Times

The channel elevation and distribution of sediment concentration can effectively reflect the erosion behavior under different operating conditions during simulation. In this study, we simulated the changes in channel elevation and sediment concentration of the measured stream flow under different operating conditions for a one-day erosion period. As shown in Figure 7a, both operating conditions 1 and 2 are in a state of sedimentation, and the sediment thickness increases with the narrowing of the channel in the transitional zone. However, at the junction between the transitional zone and the 20 m rapid channel, the increase in hydrodynamic forces causes a sudden decrease in sediment thickness, followed by an increase. The flow then gradually penetrates deeper into the channel, leading to a decrease in sediment thickness. The trend of elevation change under operating conditions 1 and 2 is consistent, but the sediment thickness under operating condition 1 is consistently higher than under operating condition 2. As shown in Figure 7b, the distribution of sediment concentration in the channel under operating conditions 1 and 2 exhibits some variations, but the sediment concentration under operating condition 1 is consistently higher than under operating condition 2 throughout the channel.

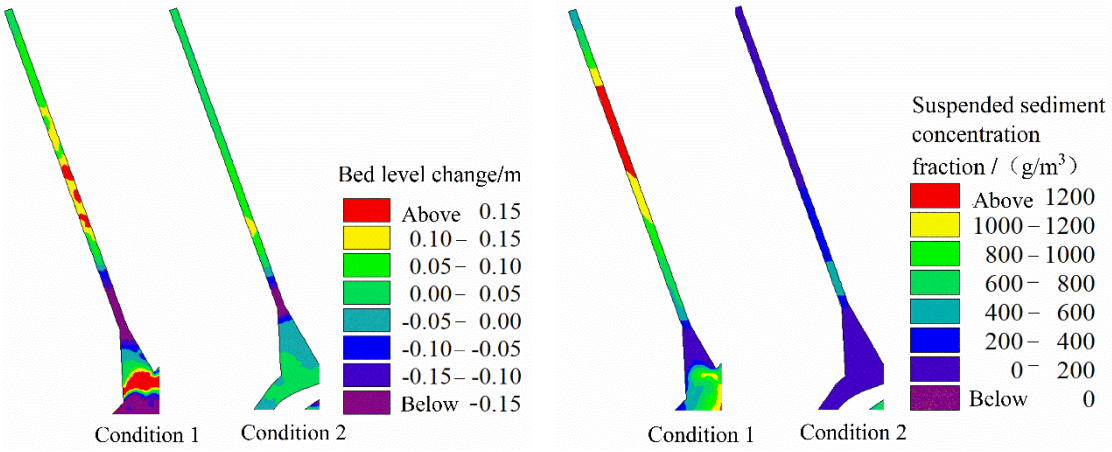

Figure 7. Erosion change map of rivers, (**a**) Elevation change map of channels; (**b**) Sediment content change map of channels.

This study conducted statistical analysis on the average height variation and sediment concentration along the channel within the study region, as illustrated in Figure 8. The maximum accumulation thickness under Condition 1 was 0.16 m, while the maximum accumulation thickness under Condition 2 was 0.115 m. The accumulation thickness was relatively similar in the area adjacent to the transitional zone and the linear segment, but the accumulation thickness in the broader region under Condition 2 was significantly lower compared to that under Condition 1. Additionally, the maximum sediment concentration under Condition 1 was 1.39 kg/m^3, which was significantly higher than the maximum sediment concentration of 0.477 kg/m^3 under Condition 2. Therefore, it can be inferred that Condition 2 effectively reduced the channel accumulation during a one-day calculation period when the flow rate was 1861.5 m^3/s.

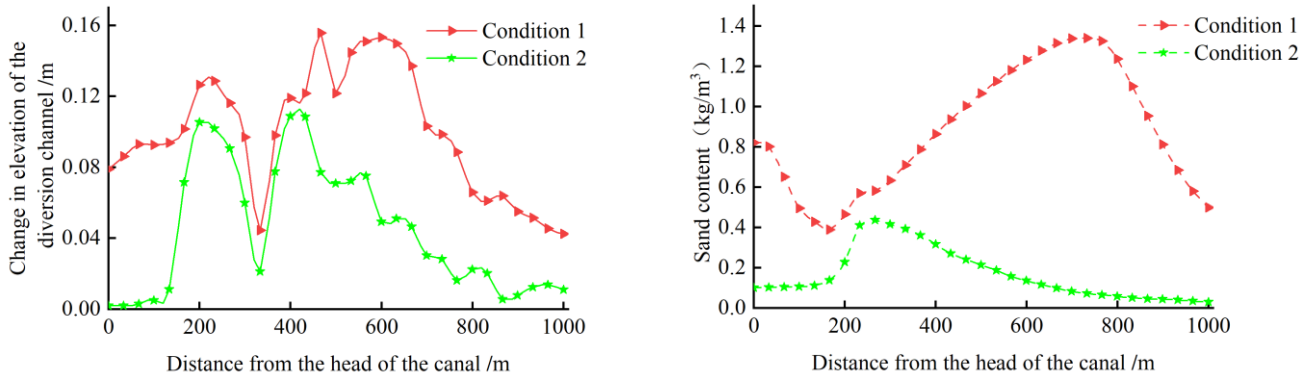

(**a**) (**b**)

Figure 8. Erosion change map of irrigation channels, (**a**) Elevation change map of irrigation channels; (**b**) Sediment content distribution map of irrigation channels.

3.3. Erosion of Diversion Channels for Different Scenarios

Based on long–term observations of water and sediment movement in the Yellow River in Ningxia, one–day erosion and sedimentation simulations were conducted for different flow scenarios (as illustrated in Figure 9). The results showed that the channel is in a state of sedimentation for all three scenarios (as illustrated in Figure 9a), with the sedimentation thickness first increasing and then decreasing. In addition, the sedimentation thickness of condition 1 is greater than that of condition 2 under the same scenario, and the sedimentation thickness of the channel increases with the increase in flow under the same condition. The maximum sedimentation thickness of condition 1 is 0.21 m in scenario 3, which is significantly larger than the maximum sedimentation thickness of 0.12 m in scenario 3 for condition 2. The minimum sedimentation thickness of condition 1 in scenario 1 is 0.003 m, but it is still larger than the minimum sedimentation thickness of 0.001 m in scenario 1 for condition 2. The sand content of the channel exhibits a similar trend to that of erosion and change (as illustrated in Figure 9b), with the maximum sand content for condition 1 being 1.74 kg/m^3 at the flow of scenario 3 and the minimum sand content being 0.38 kg/m^3 at the flow of scenario 1. The maximum sand content for condition 2 is 0.65 kg/m^3 at the flow of scenario 3, and the minimum sand content is 0.03 kg/m^3 at the flow of scenario 1. These findings suggest that condition 2 can effectively reduce the sedimentation thickness and sand content of the channel in the three scenarios to some extent.

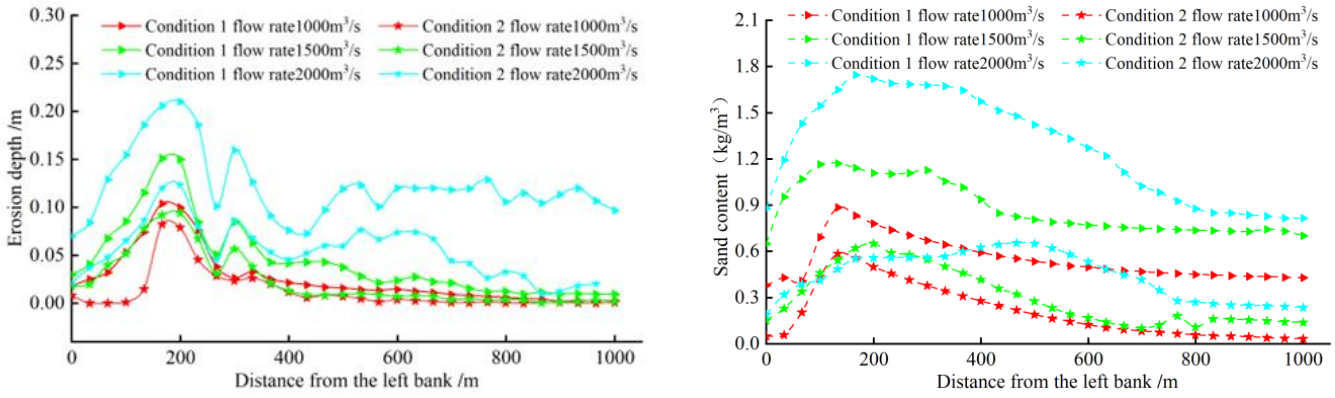

(**a**) (**b**)

Figure 9. Chart showing the changes in erosion caused by different channels in different scenarios, (**a**) Erosion depth of channels; (**b**) Graph of sediment concentration change in a channel.

3.4. Erosion of the Diversion Channel under Different Scenarios at the Same Time

In this study, the erosion characteristics of an irrigation area with long-term drainage were simulated under various operational conditions for a period of three days. The results showed that both operational conditions were in a state of sedimentation under different scenarios (as illustrated in Figure 10a). In the same scenario, the erosion thickness along the channel's straight segment exhibited a sinusoidal decline, with the sedimentation thickness of operational condition 1 being greater than that of operational condition 2 and exhibiting larger fluctuations. In scenario 3, the maximum erosion thickness and maximum erosion difference for operational conditions 1 and 2 reached their maximum values: the maximum erosion thickness for operational condition 1 was 0.37 m, with a maximum erosion difference of 0.25 m; the maximum erosion thickness for operational condition 2 was 0.28 m, with a maximum erosion difference of 0.23 m. In scenario 1, the maximum erosion thickness and maximum erosion difference for operational conditions 1 and 2 were at their minimum values: the maximum erosion thickness for operational condition 1 was 0.18 m, with a maximum erosion difference of 0.15 m; the maximum erosion thickness for operational condition 2 was 0.13 m, with a maximum erosion difference of 0.12 m. The sand content in the channel was found to vary as shown in Figure 10b, reaching a peak near the intersection of the gradient section and the straight section before decreasing steadily. The sand content was found to be similar to the value calculated for one day.

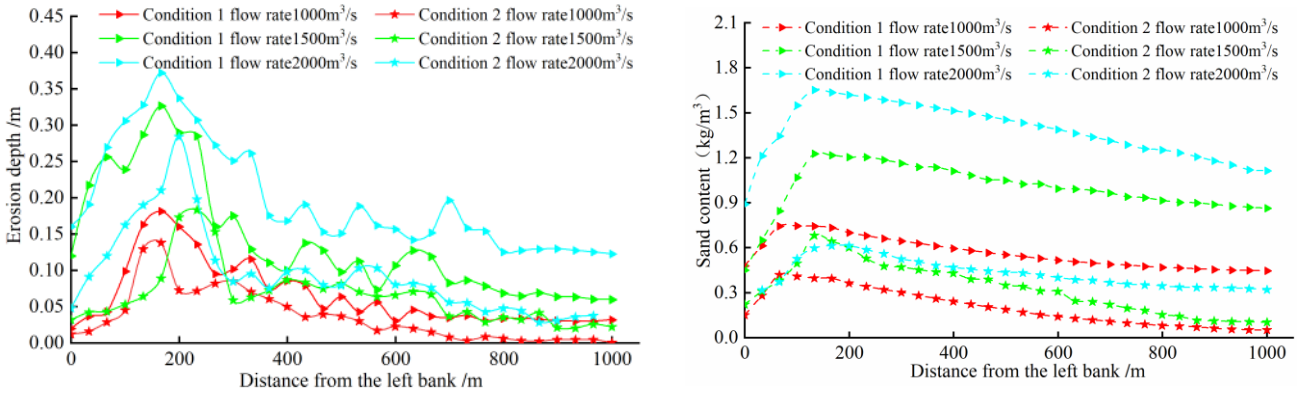

Figure 10. Chart showing the changes in erosion caused by different channels at different times and in different scenarios, (**a**) Erosion depth of channels; (**b**) Graph of sediment concentration change in a channel.

As the calculation time increases, the sediment accumulation thickness for both working conditions exhibits an upward trend, while the sediment content in the channel becomes increasingly stable.

4. Discussion

The present study performed a working condition design for the new water conveyance channel at the Shizuishan section of the Yellow River in Ningxia, China. Coupled simulation calculations were then conducted for various working conditions under various scenarios. The results showed that, compared to working condition 1, working condition 2 had three impacts on the self-irrigation area of the channel head: (1) the fishtail diverter divided and sieved the water, introducing outer river water with a lower sand content into the water supply system; (2) it decreased the flow rate of the channel head, weakening the water's sand-carrying capacity and thus reducing the sand content of the channel; and (3) it changed the hydrodynamic and erosion power changes, ultimately reducing channel sediment accumulation. The fishtail diverter in working condition 2 was found to be significantly more effective at preventing sediment accumulation and reducing sand compared to traditional Yellow River self-flow channel heads. Under scenarios 1, 2, and 3,

the maximum expected thickness was reduced by 0.05, 0.14, and 0.09 m, respectively, over a period of three days of erosion. Therefore, it can be concluded that working condition 2 can effectively improve channel sediment accumulation in the irrigation area.

Fish mouths impede the flow of streamflow to some extent [26–29], and there are significant differences in the hydrodynamic elements of the inner and outer rivers of the canal. This is due to the fact that the fish mouth causes the outer riverbed of the canal to sink, while the inner river rises. According to the principle of hydrodynamic circulation, surface water containing a small amount of sediment flows towards the concave bank, that is, towards the inner river, and enters the canal via the sand-blocking weir. On the other hand, bottom water with a high concentration of sediment flows towards the convex bank, or the outer river, and the sediment is transported into the natural river along the outer river [30,31]. However, over time, sediment will also accumulate in the inner river due to canal irrigation. The water in the inner river flows towards the sand-blocking weir with a high impact force and, due to the top-support effect, forms a vortex near the sand-throwing weir. The sediment in the water is then ejected from the sand-throwing weir and discharged into the river through the outlet. When the water volume is high, the water level will surpass the sand-throwing weir and the sediment will flow over it, exiting the outlet at a fast speed. The Dujiangyan Irrigation System employs the hydraulic design of a fish mouth to effectively manage sediment transport, thereby preventing the siltation of the Inner River and maintaining balance. This system's design has demonstrated potential for scientific research and application in various fields [25]. In addition, contemporary irrigation systems in Africa [32] as well as ancient irrigation system in the Central Negev desert [33] employ the mechanism of fish mouth structures to achieve equilibrium between water and sediment.

Therefore, in this study, we apply the aforementioned bend circulation principle to the design of the head of the canal in the self-flow irrigation area of the Yellow River in Ningxia, in order to ensure the long-term operation of the water supply system.

The MIKE 21 software is capable of simulating the movement of water and sediment with high accuracy. The two-dimensional water-sediment coupling model can accurately depict the movement state of natural rivers through a mathematical model, simulating the intricate details of the movement of hydrodynamic elements in channels and thus enabling the visualization of the temporal variation of hydrodynamic elements in the canal under different hydrological conditions. However, this study also has some limitations. Firstly, the hydrodynamic elements of the river undergo changes after the addition of the canal, and field measurements are necessary to assess the changes in the movement of the natural river under different operating conditions. Secondly, the design in this study is based on the results of numerical simulation and lacks experimental validation from actual engineering projects. Therefore, in the forthcoming work it will be necessary to monitor the actual hydrodynamic elements after the construction of the canal head under the two operating conditions to ensure that the design of operating condition 2 is effective in reducing sediment in the canal.

5. Conclusions

The current study aims to simulate the construction of a new channel in the Yellow River irrigation area using MIKE 21 modeling. Based on observed hydrodynamic data from the Shizuishan section of the Yellow River in Ningxia, a mathematical model was developed and its accuracy was verified. The design of the channel's entrance, referred to as "Work Condition 1" and "Work Condition 2", was also carried out, and simulation calculations were performed on the flow under different scenarios. The following conclusions were obtained:

1. The fish mouth design utilizes the principle of bend circulation to divide the river into inner and outer channels. The inner channel exhibits higher flow velocity and higher sediment concentration compared to the outer channel, which has lower flow velocity

and lower sediment concentration. This design effectively reduces the hydrodynamic conditions and subsequently lowers the sediment-carrying capacity of the water flow.

2. Simulation calculations using a one-day time frame reveal that under different scenarios, the maximum sediment accumulation thickness for channel condition 1 is 0.21 m, while channel condition 2 exhibits a maximum sediment accumulation thickness of 0.12 m. These results demonstrate a significant reduction in sediment for channel condition 2.
3. As erosion time increases, both channel conditions exhibit sediment accumulation. However, when the calculation time and scenarios are held constant, the sediment accumulation thickness of channel condition 1 consistently exceeds that of channel condition 2.

Therefore, after the establishment and verification of the accuracy of the physical model for channel condition 2 at the head of the channel, it can potentially be applied in the construction of the head of the self-flowing irrigation channel in the Yellow River Irrigation District.

Author Contributions: Conceptualization, M.L. and S.L.; methodology, S.L.; software, Q.Q.; validation, M.L., L.S.; formal analysis, M.L.; investigation, Q.Q.; resources, S.L.; data curation, M.L.; writing—original draft preparation, M.L.; writing—review and editing, L.S.; visualization, L.S.; supervision, S.L.; project administration, S.L.; funding acquisition, S.L. All authors have read and agreed to the published version of the manuscript.

Funding: This research was funded by Ningxia Natural Science Foundation Project (grant number 2021AAC03173).

Institutional Review Board Statement: Not applicable.

Informed Consent Statement: Not applicable.

Data Availability Statement: The data presented in this study are available on request from the corresponding author.

Acknowledgments: We would like to thank the reviewer for their valuable comments and suggestions, to the editors for their serious and responsible attitude, to the publisher for this valuable opportunity. We also thank our other colleagues for their valuable comments and suggestions that helped to improve the manuscript.

Conflicts of Interest: The authors declare no conflict of interest.

References

1. Goel, A.; Pillai, N.N. A flowmeter for rectangular irrigation field channels. *Water Manag.* **2008**, *161*, 135–139. [CrossRef]
2. Khater, A.; Kitamura, Y.; Shimizu, K.; Abou El Hassan, W.; Fujimaki, H. Quantitative analysis of reusing agricultural water to compensate for water supply deficiencies in the Nile Delta irrigation network. *Paddy Water Environ.* **2015**, *13*, 367–378. [CrossRef]
3. Outeiro, J.C.; Umbrello, D.; M'saoubi, R. Experimental and numerical modelling of the residual stresses induced in orthogonal cutting of AISI 316L steel. *Int. J. Mach. Tools Manuf.* **2006**, *46*, 1786–1794. [CrossRef]
4. Qiao, Q.; Li, C.G.; Jing, H.F.; Huang, L.X.; Yang, C. Impact of an artificial chute cutoff on the river morphology and flow structure in Sipaikou area of the Upper Yellow River. *J. Mt. Sci.* **2021**, *18*, 16. [CrossRef]
5. Surian, N. Downstream variation in grain size along an Alpine river: Analysis of controls and processes. *Geomorphology* **2002**, *43*, 137–149. [CrossRef]
6. Moussavi-Harami, R.; Mahboubi, A.; Khanehbad, M. Analysis of controls on downstream fining along three gravel-bed rivers in the Band-e-Golestan drainage basin NE Iran. *Geomorphology* **2004**, *61*, 143–153. [CrossRef]
7. Bathurst, J.C.; Carling, P.A.; Reid, I.; Walling, D.E.; Webb, B. *Sediment Erosion, Transport, and Deposition*; Wiley: Hoboken, NJ, USA, 1997.
8. Petts, G.E.; Gurnell, A.M.; Gerrard, A.J.; Hannah, D.M.; Hansford, B.; Morrissey, I.; Edwards, P.J.; Kollmann, J.; Ward, J.V.; Tockner, K.; et al. Longitudinal variations in exposed riverine sediments: A context for the ecology of the Fiume Tagliamento, Italy. *Aquat. Conserv.* **2000**, *10*, 249–266. [CrossRef]
9. Surian, N. Fluvial Processes in Braided Rivers. In *Rivers–Physical, Fluvial and Environmental Processes*; Springer: Cham, Switzerland, 2015; pp. 403–425.
10. Mueller, E.R.; Pitlick, J. Sediment supply and channel mor phology in mountain river systems: 2. Single thread tobraided transitions. *J. Geophys. Res. Earth Surf.* **2014**, *119*, 1516–1541. [CrossRef]
11. Griffiths, G.A. Sediment translation waves in braided gravel-bed rivers. *J. Hydraul. Eng.* **1993**, *119*, 924–937. [CrossRef]

12. Ashmore, P.; Bertoldi, W.; Gardner, J.T. Active width of gravelbed braided rivers. *Earth Surf. Process. Landf.* **2011**, *36*, 1510–1521. [CrossRef]
13. Bagnold, R.A. Bed load transport by natural rivers. *Water Resour. Res.* **1977**, *13*, 303–312. [CrossRef]
14. Chen, G.S.; Wang, Y.M.; Bai, T.; Du, H.H. Diagnoses of runoff-sediment relationship based on variable diagnostic method-variable step length sliding correlation coefficient method in Ning-Meng reach. *Int. J. Hydrog. Energy* **2016**, *41*, 15909–15918. [CrossRef]
15. An, C.; Lu, J.; Qian, Y.; Wu, M.; Xiong, D. The scour-deposition characteristics of sediment fractions in desert aggrading rivers—Taking the upper reaches of the Yellow River as an example. *Quat. Int.* **2019**, *523*, 54–66. [CrossRef]
16. Krishnappan, B.G.; Lau, Y.L. Turbulence Modeling of Flood Plain Flows. *J. Hydraul. Eng.* **1986**, *112*, 251–266. [CrossRef]
17. Li, J.; Fei, L.; Chen, Z.; Sun, X. Jinshan. Particle size distribution and settling velocity of sediments in water diverted from the Yellow River during border-strip irrigation. *Tecnol. Cienc. Agua* **2017**, *8*, 31–41. [CrossRef]
18. Wang, L.; Nie, Z.; Liu, M.; Cao, L.; Zhu, P.; Yuan, Q. Rational Allocation of Water Resources in the Arid Area of Northwestern China Based on Numerical Simulations. *Sustainability* **2023**, *15*, 55. [CrossRef]
19. Kim, B.J.; Hwang, J.H.; Kim, B. FLOW-3D Model Development for the Analysis of the Flow Characteristics of Downstream Hydraulic Structures. *Sustainability* **2022**, *14*, 10493. [CrossRef]
20. Wang, P.; Li, J.; Wang, M.; Hu, J.; Zhang, F. Numerical Simulation of the Hydraulic Characteristics and Fish Habitat of a Natural Continuous Meandering River. *Sustainability* **2022**, *14*, 9798. [CrossRef]
21. Soulis, V.J. Numerical Investigation of the Failure Mechanism of Articulated Aqueduct. *J. Perform. Constr. Facil.* **2018**, *32*, 1–17. [CrossRef]
22. Oyarce, P.; Gurovich, L.; Calderón, I. Simulating Hydraulic Behavior of an Agricultural Drain Based on Experimental Data. *J. Irrig. Drain. Eng.* **2017**, *143*, 1–8. [CrossRef]
23. Alomari, N.K.; Yusuf, B.; Mohammad, T.A.; Ghazali, A.H. Experimental investigation of scour at a channel junctions of different diversion angles and bed width ratios. *Catena* **2018**, *166*, 10–20. [CrossRef]
24. Zheng, X.; Kazemi, E.; Gabreil, E.; Liu, X.; Chen, R. Sustainability of the Dujiangyan Irrigation System for over 2000 Years–A Numerical Investigation of the Water and Sediment Dynamic Diversions. *Sustainability* **2020**, *12*, 2431. [CrossRef]
25. Yan, J.; Chen, M.; Xu, L.; Liu, Q.; Shi, H.; He, N. Mike 21 Model Based Numerical Simulation of the Operation Optimization Scheme of Sedimentation Basin. *Coatings* **2022**, *12*, 478. [CrossRef]
26. Tabuchi, J.P.; Aboulouard, S.; Bernier, J.; Blanchet, B.; Guérin, S.; Saint-Germain, A.; Rocher, V. The Seine river flood in June 2016, implications for the operation of the sanitation system of the heart of Paris region. *Tech. —Sci. —Methodes* **2019**, *114*, 67–80.
27. Sun, J.; Xu, N.; Ding, L.; Ma, Y.; Liu, Z.; Huang, Z. Continuous Expansions of Yangtze River Islands after The Three Gorges Dam tracked by Landsat data based on Google Earth Engine. *IEEE Access* **2020**, *8*, 92731–92742. [CrossRef]
28. Itla, B.; Jcsc, D.; Mla, B. Architecture, sedimentary facies and chronology of a composite island: A model from the Upper Paraná River, Brazil—ScienceDirect. *Geomorphology* **2020**, *372*, 107457.
29. Shi, H.; Cao, Y.; Dong, C.; Xia, C.; Li, C. The Spatio-Temporal Evolution of River Island Based on Landsat Satellite Imagery, Hydrodynamic Numerical Simulation and Observed Data. *Remote Sens.* **2018**, *10*, 2046. [CrossRef]
30. Zhang, S.; Yi, Y.; Liu, Y.; Wang, X. Hydraulic Principles of the 2,268-Year-Old Dujiangyan Project in China. *J. Hydraul. Eng.* **2013**, *139*, 538–546. [CrossRef]
31. Fan, G.; Xia, J.; Song, J.; Sun, H.; Liang, D. Research on application of ecohydrology to disaster prevention and mitigation in China: A review. *Water Supply* **2022**, *22*, 2946–2958. [CrossRef]
32. Gebrehiwot, K.A.; Haile, A.M.; De Fraiture, C.; Chukalla, A.D.; Embaye, T.G. Optimizing flood and sediment management of spate irrigation in Aba'ala Plains. *Water Resour. Manag.* **2015**, *29*, 833–847. [CrossRef]
33. Shanan, L. Runoff, Erosion, and the Sustainability of Ancient Irrigation Systems in the Central Negev Desert. In *The Hydrology-Geomorphology Interface: Rainfall, Floods, Sedimentation, Land Use*; IAHS Press: Wallingford, UK, 2000; pp. 75–106.